AMERICAN SOCIETY of
GENE & CELL
THERAPY

Liver Activation of Hepatocellular Nuclear Factor-4α by Small Activating RNA Rescues Dyslipidemia and Improves Metabolic Profile

Kai-Wen Huang,[1,2,12] Vikash Reebye,[3,12] Katherine Czysz,[3] Simona Ciriello,[3] Stephanie Dorman,[3] Isabella Reccia,[3] Hong-Shiee Lai,[1,2] Ling Peng,[5] Nikos Kostomitsopoulos,[6] Joanna Nicholls,[3] Robert S. Habib,[4] Donald A. Tomalia,[7] Pål Sætrom,[8,9] Edmund Wilkes,[10] Pedro Cutillas,[10] John J. Rossi,[11] and Nagy A. Habib[3]

[1]Department of Surgery & Hepatitis Research Center, National Taiwan University Hospital, Taipei, Taiwan, ROC; [2]Graduate Institute of Clinical Medicine, National Taiwan University College of Medicine, Zhongzheng, Taipei 10002, Taiwan, ROC; [3]Department of Surgery and Cancer, Imperial College London, London W12 0NN, UK; [4]MiNA Therapeutics Limited, London W12 0BZ, UK; [5]Centre Interdisciplinaire de Nanoscience de Marseille, 13288 Marseille, France; [6]Biomedical Research Animal Facilities, Biomedical Research Foundation of the Academy of Athens, 11527 Athens, Greece; [7]Department of Chemistry, University of Pennsylvania, Philadelphia, PA, USA; [8]Department of Cancer Research and Molecular Medicine, Norwegian University of Science and Technology, NO-7489 Trondheim, Norway; [9]Department of Computer and Information Science, Norwegian University of Science and Technology, NO-7489 Trondheim, Norway; [10]Cell Signalling and Proteomics Group, Centre for Haemato-Oncology, Barts Cancer Institute, Queen Mary University of London, London EC1M 6BQ, UK; [11]Division of Molecular Biology, Beckman Research Institute of City of Hope, Duarte, CA 91010, USA

Non-alcoholic fatty liver disease (NAFLD) culminates in insulin resistance and metabolic syndrome. Because there are no approved pharmacological treatment agents for non-alcoholic steatohepatitis (NASH) and NAFLD, different signaling pathways are under investigation for drug development with the focus on metabolic pathways. Hepatocyte nuclear factor 4-alpha (HNF4A) is at the center of a complex transcriptional network where its disruption is directly linked to glucose and lipid metabolism. Resetting HNF4A expression in NAFLD is therefore crucial for re-establishing normal liver function. Here, small activating RNA (saRNA) specific for upregulating HNF4A was injected into rats fed a high-fat diet for 16 weeks. Intravenous delivery was carried out using 5-(G5)-triethanolamine-core polyamidoamine (PAMAM) dendrimers. We observed a significant reduction in liver triglyceride, increased high-density lipoprotein/low-density lipoprotein (HDL/LDL) ratio, and decreased white adipose tissue/body weight ratio, all parameters to suggest that HNF4A-saRNA treatment induced a favorable metabolic profile. Proteomic analysis showed significant regulation of genes involved in sphingolipid metabolism, fatty acid β-oxidation, ketogenesis, detoxification of reactive oxygen species, and lipid transport. We demonstrate that HNF4A activation by oligonucleotide therapy may represent a novel single agent for the treatment of NAFLD and insulin resistance.

INTRODUCTION

Non-alcoholic fatty liver disease (NAFLD) is the most prevalent form of chronic liver disease in the world, elevating its epidemic status to that of obesity and type 2 diabetes mellitus.[1] Metabolic syndrome plays a central role in the histological progression of NAFLD, where disruption of key liver transcription factors greatly influences the natural history of this disease.

Hepatocyte nuclear factor-4 alpha (HNF4A) is a transcriptional factor expressed in the kidney, intestine, pancreatic islets cells, white adipose tissue, and liver.[2] During development, HNF4A is essential for normal liver architecture and organization of the sinusoidal endothelium. In the adult, its expression is crucial for the morphological and functional differentiation of hepatocytes, accumulation of hepatic glycogen stores, and generation of hepatic epithelium.[3] HNF4A controls the expression of numerous hepatic genes including albumin and those involved in glucose, fatty acid, cholesterol, and drug metabolism.

Two promoters expressed in different tissues drive several isoforms of HNF4A: P1 promotes the expression of isoforms 1 and 2, usually in mature hepatocytes, whereas P2 regulates the expression of isoforms 7 and 8 in the embryonic liver.[4] In this study, we focus on the expression of HNF4A driven by the P1 promoter.

The importance of HNF4A is highlighted from linkage analysis for metabolic syndrome and inflammatory bowel disease. Patients in high-risk groups with elevated serum lipid levels and chronic kidney

(legend on next page)

failure have polymorphisms in HNF4A, whereas patients with loss-of-function mutations in HNF4A have defective secretion of liver-specific proteins, such as apolipoproteins and lipoproteins.[5]

Animals lacking HNF4A have high lipid accumulation within the liver and show an impairment of liver gluconeogenesis during fasting. Loss of HNF4A reduces the secretion of serum bile acid, cholesterol, and triglycerides (TGs) levels, most likely because of defects in lipid transport and metabolism.[6] In non-alcoholic steatohepatitis (NASH) and HFD (high-fat diet)-fed diabetic models, liver expression of HNF4A is significantly reduced.[7] In rats with advanced cirrhosis, reduction in HNF4A expression correlates with worsening of liver function.[8] In view of its crucial role in regulating metabolism and proliferation, and in maintaining hepatocyte differentiation, all evidence suggests that restoration of HNF4A expression would likely be beneficial in the treatment of severe liver dysfunction such as NAFLD, liver cirrhosis, and even hepatocellular carcinoma (HCC).

With the same approach previously described,[9] we generated small activating RNA (saRNA) oligonucleotides linked with dendrimer nanoparticles. The poly(amidoamine) molecules self-assemble with saRNA to form nanoscale particles for intravenous delivery with high tropism to the liver. Here we delivered these linked saRNA nanoparticles to increase liver transcript levels of HNF4A in obese rats fed on HFD for 16 weeks. We demonstrate that enhancing liver expression of HNF4A in diet-induced NAFLD rats led to a significant improvement in serum lipids, glucose homeostasis, and body composition. HNF4A showed pleiotropic effects on genes involved in sphingolipid metabolism, fatty acid beta-oxidation, ketogenesis, detoxification of reactive oxygen species, and lipid transport.

HNF4A activation by liver-targeted oligonucleotides may represent a novel single agent in the treatment of fatty liver disease and diabetes.

RESULTS AND DISCUSSION
HNF4A-saRNA Induced HNF4A Expression in HCC Cells
To test for saRNA target activation of HNF4A, the commonly used HepG2, Hep3B, and PLCPRF5 HCC lines were transiently transfected with a mammalian-specific saRNA. A non-specific double-stranded RNA (dsRNA) (Scramble), which does not have significant homology with any known human sequences, was used as a negative control. 50 nM of double-stranded Scramble-RNA or HNF4A-saRNA was transfected into HepG2, Hep3B, and PLCPRF5 cells. HNF4A expression was evaluated 72 h later. HNF4A mRNA expression was significantly induced by HNF4A-saRNA in all three cell lines as demonstrated by quantitative RT-PCR analysis (Figure 1). HNF4A-saRNA caused a 3-fold increase in HNF4A mRNA levels (p < 0.0001) compared with untransfected HepG2 cells (Figure 1A), a 6-fold increase in Hep3B cells (p = 0.0022) (Figure 1B), and a 2-fold increase in PLCPRF5 cells (p = 0.0087) (Figure 1C). Scramble oligonucleotide did not cause an induction of HNF4A mRNA levels (Figures 1A–1C). Cell viability following saRNA transfection was also assessed by performing a WST-1 assay to confirm that hepatocytes tolerated HNF4A-saRNA transfection (Figure S1A). HNF4-saRNA was also transfected into primary rat hepatocytes showing a significant 1.5-fold increase in HNF4A mRNA expression (p = 0.03) and a 1.9-fold increase in albumin (p = 0.014) (Figures S1B and S1C). HNF4A expression at the protein level was verified by western blotting (Figure 1D). HNF4A-saRNA increased HNF4A expression 3-fold relative to untransfected control. In the presence of 10 μM rifampicin (a cytochrome p450 [CYP450] inducer), HNF4A-saRNA enhanced the ability of HepG2 cells to further increase HNF4A protein expression up to a 5-fold change when the protein bands were quantified by densitometry (Figure 1E). HNF4A-saRNA induced a 15-fold increase in albumin, which was further augmented (35-fold) upon 10 μM rifampicin treatment (Figure 1F). Protein expression of CYP3A43 increased 5.6-fold (Figure 1G) when compared with untransfected HepG2 cells. HNF4A-saRNA transfection also increased CYP450 activity as demonstrated by a luciferase assay (Figure S1D). CYP450 upregulation was measured by qPCR, where we observed a significant 1.5-fold increase in CYP3A4 (p = 0.05) (Figure 1H), a 2-fold increase in CYP3A5 (p = 0.05) (Figure 1I), and a 3.6-fold increase in CYP3A7 levels (p = 0.05) (Figure 1J).
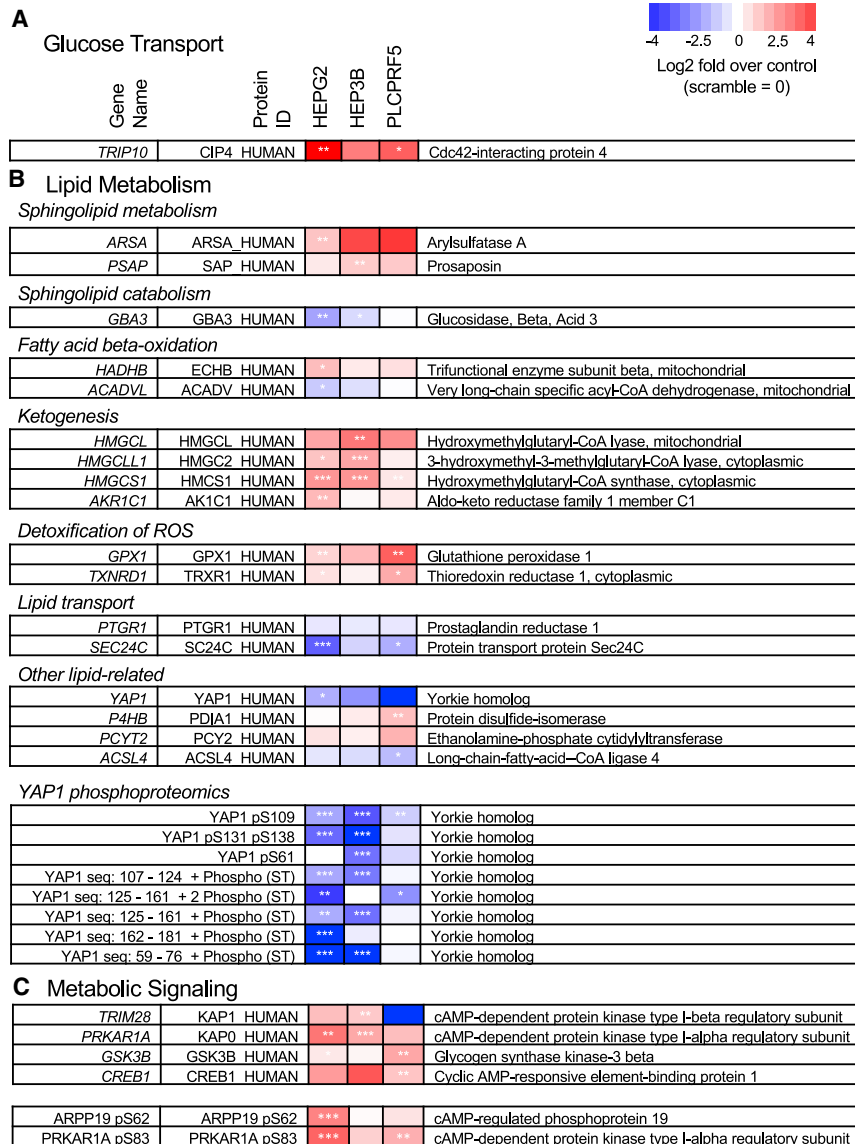
HNF4A Increases the Activity of Signaling Pathways and Transcriptional Factors Known to Promote Metabolic Regulation
Using mass spectrometry analysis of protein lysates from HNF4A-saRNA-transfected HepG2, Hep3B, and PLCPRF5 cell lines, we investigated the global protein expression and phosphoprotein changes that occurred downstream of HNF4A expression.

Over-representation analysis of the genes that showed significant protein level changes in HNF4A-saRNA-treated cell lines was enriched for pathways that regulate glucose transport (Figures 2A, lipid metabolism, and 2B; Figure S2) and energy production (Figure 2C). A search tool for the retrieval of interacting protein-protein interaction (STRING) using the top 18 enriched proteins demonstrated a strong interaction with HNF4A that linked with metabolism of lipids and glucose signaling pathways (Figure S3).

Figure 1. HNF4A-saRNA Induced Effects on Hepatocytes
(A–C) HepG2 (A), Hep3b (B), and PLCPRF5 (C) cells were transfected with HNF4A-saRNA or Scramble-RNA. Seventy-two hours after the second transfection, cells were harvested and RNA extracted. HNF4A-PR1 was normalized to GAPDH. Statistical significance compared with control: *p < 0.05; **p < 0.01; ***p < 0.0001 (two-tailed t test, 95% confidence interval). (D) Top: schematic representation of transfection protocol and rifampicin treatment. Bottom: protein extracts analyzed for CYP3A43, ALBUMIN, HNF4A, and HSP90 expression. (E–G) Quantification of western blot in (D) for protein expression levels of HNF4A (E), Albumin (F) and CYP3A43 (G). HSP90 was used a housekeeping gene. (H–J) HepG2 cells treated with DMSO or rifampicin and transfected with sa-HNF4-RNA or Scramble-RNA. Seventy-two hours after second transfection, cells were harvested and RNA extracted. CYP3A4 (H), CYP3A5 (I), and CYP3A7 (J) were normalized to actin. Asterisks denote significance as follows: *p < 0.05 (one-tailed t test, 95% confidence interval); all data represents mean ± (SEM).

A Glucose Transport

Log2 fold over control (scramble = 0), scale -4, -2.5, 0, 2.5, 4

Gene Name	Protein ID	HEPG2	HEP3B	PLCPRF5	Description
TRIP10	CIP4_HUMAN	**		*	Cdc42-interacting protein 4

B Lipid Metabolism

Sphingolipid metabolism

Gene Name	Protein ID	HEPG2	HEP3B	PLCPRF5	Description
ARSA	ARSA_HUMAN	**			Arylsulfatase A
PSAP	SAP_HUMAN		**		Prosaposin

Sphingolipid catabolism

| *GBA3* | GBA3_HUMAN | ** | | | Glucosidase, Beta, Acid 3 |

Fatty acid beta-oxidation

| *HADHB* | ECHB_HUMAN | * | | | Trifunctional enzyme subunit beta, mitochondrial |
| *ACADVL* | ACADV_HUMAN | | | | Very long-chain specific acyl-CoA dehydrogenase, mitochondrial |

Ketogenesis

HMGCL	HMGCL_HUMAN		**		Hydroxymethylglutaryl-CoA lyase, mitochondrial
HMGCLL1	HMGC2_HUMAN	*	***		3-hydroxymethyl-3-methylglutaryl-CoA lyase, cytoplasmic
HMGCS1	HMCS1_HUMAN	***	***		Hydroxymethylglutaryl-CoA synthase, cytoplasmic
AKR1C1	AK1C1_HUMAN	**			Aldo-keto reductase family 1 member C1

Detoxification of ROS

| *GPX1* | GPX1_HUMAN | ** | | ** | Glutathione peroxidase 1 |
| *TXNRD1* | TRXR1_HUMAN | | | * | Thioredoxin reductase 1, cytoplasmic |

Lipid transport

| *PTGR1* | PTGR1_HUMAN | | | | Prostaglandin reductase 1 |
| *SEC24C* | SC24C_HUMAN | *** | | * | Protein transport protein Sec24C |

Other lipid-related

YAP1	YAP1_HUMAN	*			Yorkie homolog
P4HB	PDIA1_HUMAN			**	Protein disulfide-isomerase
PCYT2	PCY2_HUMAN				Ethanolamine-phosphate cytidylyltransferase
ACSL4	ACSL4_HUMAN			*	Long-chain-fatty-acid--CoA ligase 4

YAP1 phosphoproteomics

		HEPG2	HEP3B	PLCPRF5	Description
	YAP1 pS109	***	***	**	Yorkie homolog
	YAP1 pS131 pS138	***	***		Yorkie homolog
	YAP1 pS61		***		Yorkie homolog
	YAP1 seq: 107 - 124 + Phospho (ST)	***	***		Yorkie homolog
	YAP1 seq: 125 - 161 + 2 Phospho (ST)	**		*	Yorkie homolog
	YAP1 seq: 125 - 161 + Phospho (ST)	***			Yorkie homolog
	YAP1 seq: 162 - 181 + Phospho (ST)	***			Yorkie homolog
	YAP1 seq: 59 - 76 + Phospho (ST)	***	***		Yorkie homolog

C Metabolic Signaling

Gene Name	Protein ID	HEPG2	HEP3B	PLCPRF5	Description
TRIM28	KAP1_HUMAN		**		cAMP-dependent protein kinase type I-beta regulatory subunit
PRKAR1A	KAP0_HUMAN	**	*		cAMP-dependent protein kinase type I-alpha regulatory subunit
GSK3B	GSK3B_HUMAN			**	Glycogen synthase kinase-3 beta
CREB1	CREB1_HUMAN			**	Cyclic AMP-responsive element-binding protein 1

	ARPP19 pS62	***			cAMP-regulated phosphoprotein 19
	PRKAR1A pS83	***		**	cAMP-dependent protein kinase type I-alpha regulatory subunit

Figure 2. Protein Expression and Phosphoprotein Changes Are Displayed as a Heatmap for HNF4A-saRNA-Treated Cell Lines (HepG2, Hep3B, and PLCPRF5)

Increases (red) and decreases (blue) in protein levels are displayed as the log2 fold over the scramble control, which was set at 0 (n = 3). Proteins that showed significant changes in pathways related to (A) glucose transport, (B) lipid metabolism, and (C) metabolic signaling are displayed. Asterisks denote significance as follows: $*p < 0.05$, $**p < 0.01$, $***p < 0.001$.

increase in liver size in adult mice, an effect that was, however, reversible upon inhibition of YAP1 expression.[11]

We also observed an increase in the expression of protein kinases in metabolic signaling pathways (Figure 2C). These included glycogen synthase kinase-3 beta (GSK3β) and two isoforms of cAMP-dependent protein kinase A (PKA) regulatory subunits (PRKAR1A and PRKAR1B), as well as cAMP-responsive element-binding protein 1 (CREB1). Reduction of these factors is held accountable for the pathophysiological changes that cause NAFLD.[12]
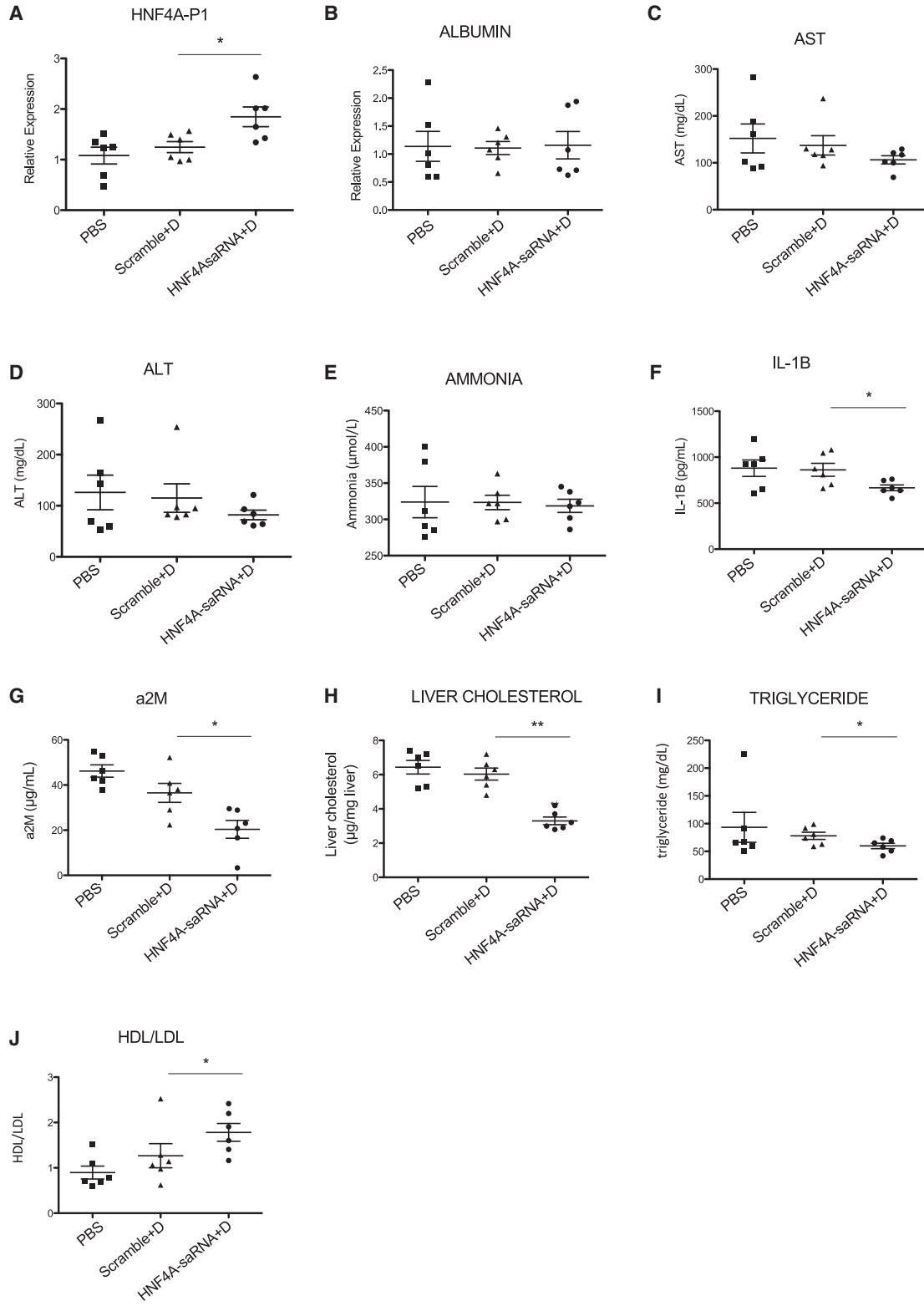
HNF4A-saRNA-Dendrimer Treatment Increases Liver Expression of HNF4A

Because upregulation of HNF4A by saRNA caused predicted changes in lipid and cholesterol metabolic pathways, we next sought to investigate the physiological effects of delivering therapeutic amounts of HNF4A-saRNA-dendrimer (0.6 mg/kg) or Scramble oligonucleotide control (Scramble-dendrimer) into a rat model sustained on an HFD. PAMAM dendrimer complex with saRNA for intravenous delivery has previously been validated by our group.[9] Eighteen male Wistar rats (6–8 weeks old) were fed for 16 weeks with HFD. The animals were divided into three groups of six animals each. Groups 1–3 were injected at days 1, 3, 5, 12, and 17. The control group 1 was injected with 600 µL of PBS, control group 2 with 600 µL Scramble-dendrimer, and experimental group 3 with 600 µL HNF4A-saRNA-dendrimer. Blood samples were collected at day 22 prior to animal sacrifice for analysis. The liver lobes were immediately extracted at the end of the study. Each resected liver lobe within the groups were divided into two sections, one for flash freezing (for RNA isolation) and the second for formalin fixing followed by paraffin embedding (Figure S4A).

To confirm target engagement of the saRNA in the liver samples, we analyzed total RNA from tissue sections for HNF4A transcript expression using HNF4A-P1 promoter-specific FAM-labeled probes.

We observed increased protein expression in genes involved in fatty acid β-oxidation and ketogenesis. Our observed changes in liver TG levels (Figure 3I) concurrent to *in vitro* changes in mediators of lipid transport P4HB and SEC24C (Figure S2) have also previously been documented in an HFD-fed animal study where a decrease in fatty acid β-oxidation was proposed to contribute to hepatic lipid accumulation, whereas ketogenesis was reported to prevent fatty liver injury and hyperglycemia.[10] P4HB is involved in hepatic very low-density lipoprotein (VLDL) assembly and lipid homeostasis, whereas SEC24C is the rate-limited step in transporting dietary fat across the intestinal absorptive cells. A reduction in protein expression of YAP1 and dephosphorylation at multiple sites was also observed across all HNF4A-saRNA-treated cell lines (Figure 2B). YAP1 is a downstream target of the Hippo signaling pathway and is thought to play a role in organ size. Prolonged activation of YAP1 has been shown to lead to an

A HNF4A-P1

B ALBUMIN

C AST

D ALT

E AMMONIA

F IL-1B

G a2M

H LIVER CHOLESTEROL

I TRIGLYCERIDE

J HDL/LDL

(legend on next page)

A 1.5-fold increase in HNF4A transcript was detected from the treated liver relative to Scramble control (p = 0.0411) (Figure 3A). No change in albumin transcript levels was detected across each of the treatment groups, suggesting that either there was no pathological requirement for albumin release from the animals, or that steady-state levels of albumin were simply maintained through a feedback regulation that is known to occur in rats (Figure 3B). No significant changes in liver function parameters (aspartate aminotransferase [AST], alanine aminotransferase [ALT], and ammonia), including albumin, were observed when measured on a VITROS FS ELISA platform, indicating that HNF4A-saRNA-dendrimer injections caused no liver-specific contraindications (Figures 3C–3E). When circulating markers of inflammation were measured from the treated rats, we observed a significant 1.3-fold reduction in interleukin-1 beta (IL-1β; p = 0.0411) (Figure 3F), suggesting a reduction in inflammation, and a 1.8-fold decrease in alpha-2 macroglobulin (a2M; p = 0.0260) (Figure 3G), suggesting a decrease in at least one of the factors that contribute to insulin resistance. No abnormal changes in white blood cells (WBCs) were observed (Figures S4C and S4D).

HNF4A Effect on Serum Lipid Profile

HNF4A-saRNA-dendrimer treatment significantly reduced levels of liver cholesterol by over 40% (p = 0.0022; Figure 3H) in treated animals compared with the control groups despite the animals continuously being fed an HFD. Furthermore, we observed a 1.3-fold reduction in liver TG (p = 0.0388; Figure 3I) and 1.4-fold increase in HDL/LDL ratio in the treated animals (p = 0.0465; Figure 3J). This correlates very well with humans where normalization of the HDL/LDL ratio is seen with a dyslipidemic diet. FFPE tissue sections were processed and stained with hematoxylin and eosin (H&E) for ultrastructural observation of fat deposits. H&E staining appeared more fulminant in the HNF4A-saRNA-treated groups when compared with the control groups (PBS and Scramble) where punctate unstained areas were observed (Figure 4A). Loss in total body weight was also significantly greater by 3.5-fold in the HNF4A-saRNA-dendrimer-treated groups when compared with untreated control (p = 0.0263) (Figure 4B). The white adipose tissue/body weight and the liver/body weight ratios also showed a significant 1.15-fold decrease and 1.2-fold decrease, respectively, in the HNF4A-saRNA-dendrimer-treated animals (p = 0.0411 and p = 0.0260, respectively) (Figures 4C and 4D). No significant reduction in pancreas weight and brown fat content was noted (Figures S4C and S4D).

HNF4A Normalized Glucose Homeostasis

HNF4A-saRNA-dendrimer treatment caused a significant 1.3-fold decrease in serum glucose levels when compared with the control groups (p = 0.0129) (Figure 3E). Circulating insulin level was not affected by HNF4A-saRNA (Figure 4F), indicating that glucose clearance by pancreatic secretion of insulin was unlikely. Reducing IL-6 levels (Figure 4G) and a 1.9-fold decrease in TG/HDL ratio (p = 0.0411) (Figure 4H) suggest improved metabolic profile, which likely contributes to decreased insulin resistance following HNF4A-saRNA treatment.

In summary, NAFLD encompasses a wide spectrum of histology from asymptomatic hepatic steatosis to cirrhosis. In the absence of liver inflammation or fibrosis, most patients with NAFLD have simple steatosis. The progression of NAFLD to NASH is of great significance because it can evolve to cirrhosis, liver failure, and HCC. Obesity, diabetes, and insulin resistance are the crucial risk factors for the progression of NASH. It is therefore vital to understand the key factors that are central to lipid and glucose metabolism in order to prevent or manage progression of NASH. HNF4A is at the center of a complex network of transcriptional control where its disruption has directly been linked to several human diseases including diabetes and steatosis.[5] Insight into the transcription regulatory network of HNF4A highlights the importance of this transcription factor in regulating liver-specific genes involved in glucose, cholesterol, and fatty acid metabolism.

In this study, we demonstrated the importance of resetting the transcriptional network of HNF4A with HNF4A-saRNA in a NAFLD rat model where TG biosynthesis, phospholipid metabolism, and arachidonic acid metabolism network were engaged (Figure 4I).

Analysis of the global phosphoprotein changes caused by HNF4A-saRNA showed significant alteration to glucose transport and insulin resistance.

Glucose Transport

Regulation of ARSA, PSAP, GBA3, and CDC42 interacting protein 4 by HNF4A in hepatocytes suggested that more efficient glucose transport contributed to the decrease in glucose serum level in the HNF4A-saRNA-treated animals.

Insulin Resistance

Regulation of factors for lipid transport (P4HB and SEC24C), lipid metabolism (YAP1), and oxidation of fatty acid (HADHB, ACADVL) by HNF4A-saRNA, together with reduction in IL-6, liver cholesterol, liver TG, HDL/LDL ratio, and TG/HDL ratio, all point toward HNF4A-saRNA-induced increase in HNF4A reducing insulin resistance.

HNF4A-saRNA treatment in a model of fatty liver disease (HFD-fed animal) caused changes in a collective network of factors that

---

Figure 3. The Effects of HNF4-saRNA Treatment in the Liver and Blood of HFD Rats

(A and B) RNA extracted from liver tissue was analyzed for (A) HNF4A-P1 and (B) albumin expression. HNF4A-PR1 was normalized to HPRT. Albumin was normalized to GAPDH. (C–E) Serum levels of (C) aspartate aminotransferase (AST), (D) alanine aminotransferase (ALT), and (E) ammonia showed no significant change upon HNF4A-saRNA treatment. (F and G) Interleukin-1 beta (IL-1β) (F) and alpha-2 macroglobulin (a2M) (G) showed a significant reduction. (H–J) Liver cholesterol (H), triglyceride (I), and HDL/LDL (J) changes upon HNF4A-saRNA treatment. Asterisks denote significance as follows: *p < 0.05 (two-tailed t test, 95% confidence interval); mean ± (SEM).
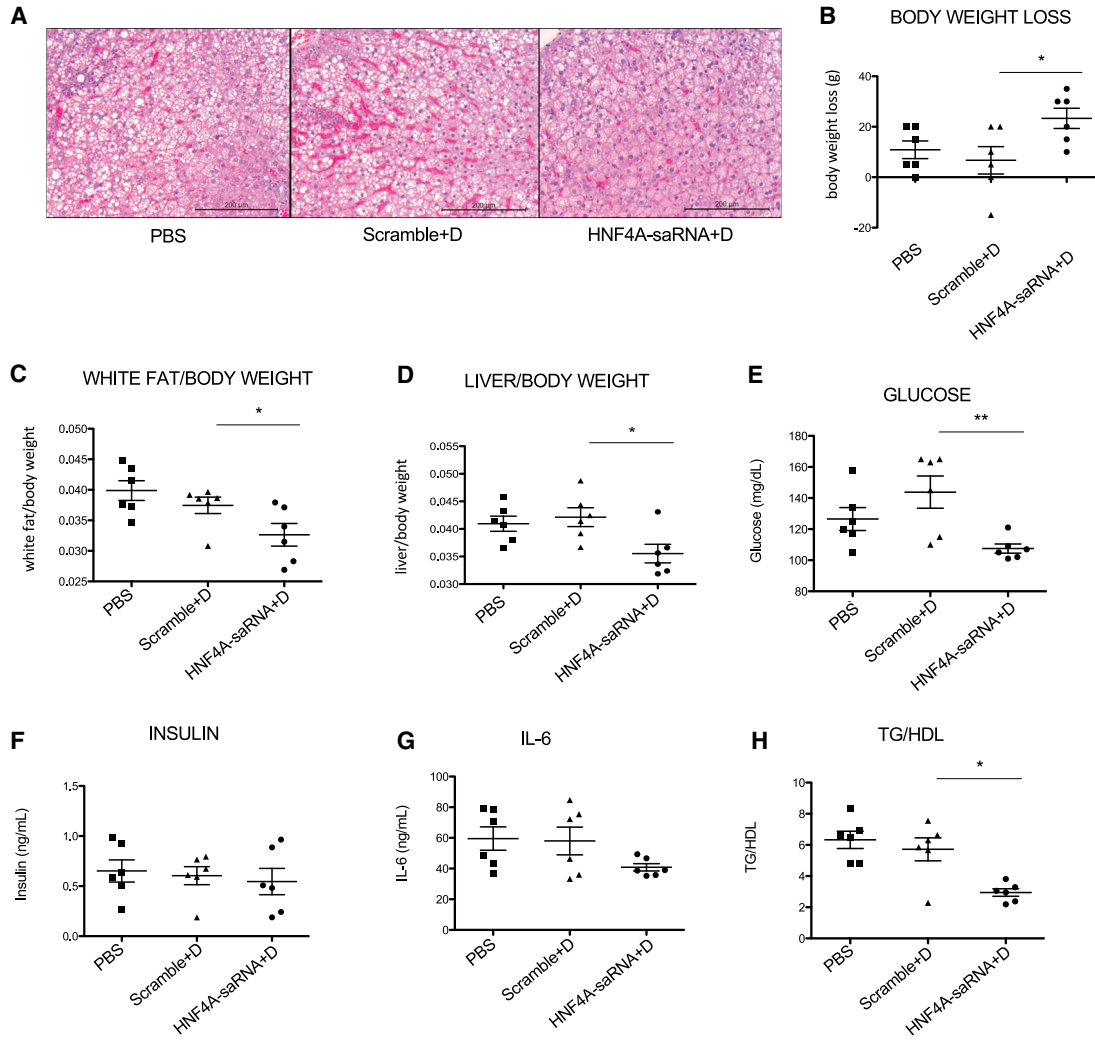
I. Lipid metabolism in the context of the liver
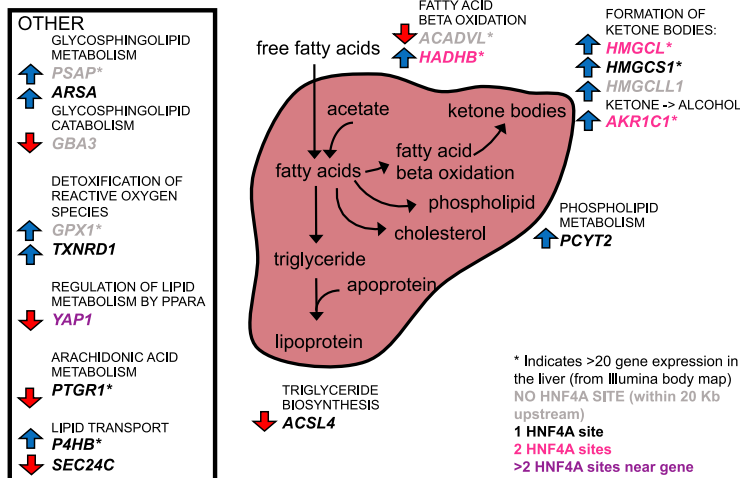
(legend on next page)

culminated in significant improvement in the metabolic profile. Because there are no approved pharmacological treatment agents for NASH and NAFLD, management entails a multi-targeted approach with several drugs and even surgery to treat the metabolic risk factors and improve insulin sensitivity.

We demonstrate that activation of HNF4A by saRNA/nanoparticle conjugates may represent a novel single agent in the treatment or management of fatty liver disease and insulin resistance.

MATERIALS AND METHODS
All authors had access to these study data, and reviewed and approved the final manuscript.

Design of saRNA Oligonucleotides and Transfection
The design for selecting saRNA for targeted gene activation has been previously described by our group.[9]

Dendrimer-Based siRNA Delivery *In Vivo*
The G5 dendrimer was synthesized starting with the triethanolamine core and following the iterative "addition" and "amidation" method as previously described.[9] To form HNF4A-saRNA-G5 coated dendrimer complexes, the dendrimers were mixed with saRNAs at a ratio of 5:1 (dendrimer : saRNA) and incubated at 37C for 30min. The resulting complexes were then injected intravenously. (Note G5 here refers to the 5th generation of PAMAM dendrimers containing 96 end-amine groups).

Animal Model, Experimental Design, and Sample Collection
The animals used for this study were 6- to 8-week-old male Wistar rats. This study was approved by the University of Taiwan animal welfare committee. In order to induce the HFD phonotype, the animals were fed for 16 weeks with HFD consisting of 83% standard diet (Catalog Number [Cat. No.] 5001; LabDiet), 15% lard oil (Cat. No. L0657; Sigma), and 2% cholesterol (Cat. No. C8503; Sigma). Animals were housed in groups of three per cage in the vivarium for the duration of the experiment. Standard controlled environment of 22°C ± 3°C, 50% ± 20% humidity, and night/dark cycle of 12 h every day was maintained with 15–20 fresh air changes per hour. Eighteen male Wistar rats of 300 ± 20 g body weight were obtained from the animal center of National Taiwan University. The rats were fed a high-fat and high-cholesterol diet for 16 weeks. At 16 weeks, rats were randomized into three groups and injected via tail vein with either PBS, 0.6 mg/kg of HNF4A saRNA + dendrimer (HNF+D), or 0.6 mg/kg of Scramble saRNA + dendrimer (SC+D), in 600 μL of PBS final volume. Animals were

injected three times per week at week 1 followed by one injection every 2 weeks. At week 19, the animals were weighed and euthanized. Blood samples were collected; the liver and pancreas were removed, weighed, and processed for downstream analysis (RNA extraction, formaldehyde fixed, and paraffin embedded). White and brown fat content were also evaluated. The liver, pancreas, and fat weight are expressed in relation to the total body weight.

Serum Biochemical Profiles
Serum levels of ALT, AST, cholesterol, TG, HDL, LDL, ammonia, WBCs, glucose, insulin, a2M, IL-1β, and IL-6 were measured with VITROS 5.1 FS Chemistry Systems (Ortho-Clinical Diagnostics). For lipid analysis, blood samples were collected for the determination of total cholesterol and TG content using commercial kits (Sigma, St. Louis, MO, USA). Insulin resistance was evaluated through the TG/HDL ratio. A TG/HDL ratio ≥3 is considered as an index of insulin resistance. The following ELISA kits were used according to the manufacturer's protocol: Rat Insulin, Mercodia Cat. No. 10-1250-01; Rat IL-1 beta, RayBiotech Cat. No. ELR-IL1b; Rat Alpha-2-Macroglobulin, Cloud-Clone Cat. No. SEB017Ra; Rat IL-6, Cloud-Clone Cat. No. SEA079Ra; Rat TNF-a, BioLegend Cat. No. 438207; and Rat Albumin, Bethyl Laboratories, Cat. No. E110-125.

Liver Lipid Extraction and Quantification
For liver cholesterol measurement, 10 mg liver tissue was extracted with 200 μL of chloroform/isopropanol/Nonidet P-40 (NP-40; 7:11:0.1). Cholesterol extracted from liver was quantified enzymatically using a Cholesterol/Cholesteryl Ester Quantitation Kit (K603-100; Biovision) following the manufacturer's instructions.

For TGs extraction, tissues (∼100 mg) were homogenized in 1 mL water solution containing 5% NP-40. After a slow heat-up to 80°C–100°C in the water bath, samples were maintained in the water bath for 2–5 min or until the NP-40 became cloudy, then cooled down to room temperature. The heating was subsequently repeated. The samples were then centrifuged for 2 min at top speed in a microcentrifuge to remove any insoluble material. TGs extracted from liver were quantified enzymatically using a Triglycerides Quantitation Kit (K622-100; Biovision) following the manufacturer's instructions.

Histology
Samples from liver were fixed in 10% phosphate-buffered formalin, embedded in paraffin, and stained with H&E.

Figure 4. The Effects of HNF4-saRNA Treatment in HFD Rats and Its Consequence on Lipid Metabolism

(A–D) H&E staining of paraffin-embedded liver section (A), animal body weight loss (B), white fat body weight ratio (C), and liver body weight ratio (D) after treatment. (E–H) Serum glucose (E), insulin (F), interleukin-6 (IL-6) (G), and TG/HDL ratio (H) after treatment. Asterisks denote significance as follows: *p < 0.05, **p < 0.01 (in A, F–H, and K, two-tailed t test, 95% confidence interval); mean ± (SEM). (B, C, and E) One-tailed t test, 95% confidence interval. (I) Genes showing significant increase or decrease in expression in HNF4A-saRNA-treated cells lines are depicted in the context of lipid metabolism in the liver. Blue "up" arrows indicate increases and red "down" arrows indicate decreases were observed in the expression of protein products of the genes (from Figure 2). Asterisks note genes that have levels of expression >20 in the liver (according to the Illumina Body Map), and the color of the gene names correspond with the presence of HNF4a binding sites upstream of the gene (see Figure S1 for further details).

Table 1. SYBR Probes and FAM-Labeled Probes Used for Transcript Levels Analysis

PROBE NAME	CATALOGUE NUMBER	MANUFACTURER
ACTB_1_SG	QT00193473	QIAGEN
ALB_1_SG	QT00189679	QIAGEN
CEBPA_1_SG	QT00395010	QIAGEN
HNF4A_1_SG	QT00188223	QIAGEN
GAPD_1_SG	QT00199633	QIAGEN
HNF4A-P1	Rn 00696984m1	Applied Biosystems
HPRT	Rn 01526840m1	Applied Biosystems

Proteomics Analysis

Phosphoproteomics experiments were performed using mass spectrometry as previously reported.[13] In brief, cells were lysed in urea lysis buffer (8M urea, 10 mM Na_3VO_4, 50 mM NaF, 100 mM β-glycerol phosphate, and 25 mM $Na_2H_2P_2O_7$), and proteins reduced and alkylated by sequential addition of 1 mM DTT and 5 mM iodoacetamide. Immobilized trypsin was then added to digest proteins into peptides. After overnight incubation with trypsin, peptides were desalted by solid-phase extraction (SPE) using OASIS HLB columns (Waters) in a vacuum manifold following manufacturer's guidelines with the exception that the elution buffer contained 1M glycolic acid. Phospho-peptides were enriched from the resulting peptide mixture using TiO_2 chromatography with the modifications described by Montoya.[14] TiO_2 chromatographic media were added to the SPE eluted peptides and incubated 5 min with rotation. The TiO_2 media were then packed in empty spin-tips and washed three times with 1M glycolic acid, 5% trifluoroacetic acid (TFA). Phospho-peptides were eluted with 5% NH_4OH and dried in a vacuum concentrator.

Dried phospho-peptide extracts were dissolved in 0.1% TFA and analyzed by nanoflow liquid chromatography-tandem mass spectrometry (LC-MS/MS) in an LTQ-orbitrap as described before.[13] Gradient elution was from 2% to 35% buffer B in 90 min with buffer A (0.1% formic acid in water and buffer B was 0.1% formic acid in acetonitrile) being used to balance the mobile phase. MS/MS was acquired in multistage acquisition mode. MS raw files were converted into Mascot Generic Format using Mascot Distiller (version 1.2) and searched against the SwissProt database (Database: 2013.03) restricted to human entries using the Mascot search engine (version 2.3). Allowed mass windows were 10 ppm and 600 mmu (millimass units) for parent and fragment mass-to-charge values, respectively. Variable modifications included in searches were oxidation of methionine, pyro-glu (N-term), and phosphorylation of serine, threonine, and tyrosine. Results were filtered to include those with a potential for false discovery rate less than 1% by comparing with searches against decoy databases. Quantification was performed by obtaining peak areas of extracted ion chromatographs (XICs) for the first three isotopes of each peptide ion using Pescal.[15] Mass and retention time windows of XICs were 7 ppm and 1.5 min, respectively.

Transfection Reaction

For analyzing gene activation and protein expression, hepatocytes were seeded into 24-well plates at a density of 1×10^5 cells/well. Transfection was performed with Lipofectamine 2000 following the manufacturer's instructions (Cat. No. 11668019; Life Technologies). HNF4A-saRNAs or Scramble saRNAs were added to the cells at a final concentration of 50 nM. Transfection was repeated 24 h later, and the cells were harvested at the 72-h time point. All experiments with rifampicin were treated at a final concentration of 10 μM.

RNA Extraction

Total RNA was extracted for reverse transcription (QuantiFast Reverse transcription; QIAGEN) and target cDNA amplification by real-time PCR (QuantiFast SYBR Green Master mix). The cDNA probes used are listed below using QuantiTect SYBR Probes from QIAGEN.

Real-Time PCR Probes

Real-time PCR was performed with the SYBR/FAM probes according to the manufacturer (QIAGEN, Applied Biosystems) (Table 1).

Protein Extraction for Western Blotting

Total protein was extracted using a conventional radioimmunoprecipitation assay (RIPA) buffer (50 mM Tris-HCl, 150 mM sodium chloride, 1.0% Igepal, 0.5% sodium deoxycholate, and 0.1% SDS). The total protein content was then quantitated using a Bradford assay, following the manufacturer's instructions (Bio-Rad). Total protein extracts were separated by SDS-PAGE and transferred onto polyvinylidene fluoride (PVDF) membranes, then were probed with antibodies against HNF4A (Cat. No. ab92378; Abcam), CYP3A4 (Cat. No. ab124921; Abcam), albumin (Cat. No. ab131176; Abcam), and heat shock protein 90 (HSP90; Cat. No. SPA-846; Stressgene). The proteins of interest were detected with a horseradish peroxidase (HRP)-conjugated secondary antibody (1:5000) and visualized with LI-COR Western Sure ECL substrate, according to the manufacturer's protocol.

Luciferase Assay

Luciferase assays were carried out according to the manufacturer's instructions (Promega p450-Glo, TB325).

Data Analysis

All values were represented as a mean ± standard error or mean (SEM). Statistical comparison between groups was done using the Student's t test, confidence interval 95%; $p < 0.05$ was considered to be statistically significant (SPSS version 17.0; IBM Corporation, Armonk, NY, USA).

SUPPLEMENTAL INFORMATION

Supplemental Information can be found online at https://doi.org/10.1016/j.omtn.2019.10.044.

AUTHOR CONTRIBUTIONS

K.-W.H., V.R., and N.A.H. designed the experiments. V.R. and K.C. performed the cellular experiments and analyzed the data. S.C.

analyzed liver tissue samples. S.D. analyzed proteomics array and performed gene ontology analysis. K.-W.H. and H.-S.L. performed the *in vivo* study. P.S. designed HNF4-sa RNA. P.C. and E.W. performed global proteomics array. V.R., K.-W.H., and N.A.H. wrote the manuscript. J.N. and R.S.H. managed execution of this study. S.C., S.D., I.R., J.J.R., L.P., N.K., and D.A.T. contributed to editing the manuscript.

CONFLICTS OF INTEREST

N.H., J.R., R.H., J.N., and V.R have equity in MiNA Therapeutics Limited. All remaining authors have no conflicts to declare.

REFERENCES

1. NCD Risk Factor Collaboration (NCD-RisC) (2016). Trends in adult body-mass index in 200 countries from 1975 to 2014: a pooled analysis of 1698 population-based measurement studies with 19·2 million participants. Lancet *387*, 1377–1396.

2. Harries, L.W., Brown, J.E., and Gloyn, A.L. (2009). Species-specific differences in the expression of the HNF1A, HNF1B and HNF4A genes. PLoS One *4*, e7855.

3. Parviz, F., Matullo, C., Garrison, W.D., Savatski, L., Adamson, J.W., Ning, G., Kaestner, K.H., Rossi, J.M., Zaret, K.S., and Duncan, S.A. (2003). Hepatocyte nuclear factor 4alpha controls the development of a hepatic epithelium and liver morphogenesis. Nat. Genet. *34*, 292–296.

4. Torres-Padilla, M.E., Fougère-Deschatrette, C., and Weiss, M.C. (2001). Expression of HNF4alpha isoforms in mouse liver development is regulated by sequential promoter usage and constitutive 3′ end splicing. Mech. Dev. *109*, 183–193.

5. Weissglas-Volkov, D., Huertas-Vazquez, A., Suviolahti, E., Lee, J., Plaisier, C., Canizales-Quinteros, S., Tusie-Luna, T., Aguilar-Salinas, C., Taskinen, M.R., and Pajukanta, P. (2006). Common hepatic nuclear factor-4alpha variants are associated with high serum lipid levels and the metabolic syndrome. Diabetes *55*, 1970–1977.

6. Krapivner, S., Iglesias, M.J., Silveira, A., Tegnér, J., Björkegren, J., Hamsten, A., and van't Hooft, F.M. (2010). DGAT1 participates in the effect of HNF4A on hepatic secretion of triglyceride-rich lipoproteins. Arterioscler. Thromb. Vasc. Biol. *30*, 962–967.

7. Yue, H.-Y., Yin, C., Hou, J.-L., Zeng, X., Chen, Y.X., Zhong, W., Hu, P.F., Deng, X., Tan, Y.X., Zhang, J.P., et al. (2010). Hepatocyte nuclear factor 4alpha attenuates hepatic fibrosis in rats. Gut *59*, 236–246.

8. Liu, L., Yannam, G.R., Nishikawa, T., Yamamoto, T., Basma, H., Ito, R., Nagaya, M., Dutta-Moscato, J., Stolz, D.B., Duan, F., et al. (2012). The microenvironment in hepatocyte regeneration and function in rats with advanced cirrhosis. Hepatology *55*, 1529–1539.

9. Reebye, V., Sætrom, P., Mintz, P.J., Huang, K.W., Swiderski, P., Peng, L., Liu, C., Liu, X., Lindkaer-Jensen, S., Zacharoulis, D., et al. (2014). Novel RNA oligonucleotide improves liver function and inhibits liver carcinogenesis in vivo. Hepatology *59*, 216–227.

10. Nagle, C.A., Klett, E.L., and Coleman, R.A. (2009). Hepatic triacylglycerol accumulation and insulin resistance. J. Lipid Res. *50* (*Suppl*), S74–S79.

11. Camargo, F.D., Gokhale, S., Johnnidis, J.B., Fu, D., Bell, G.W., Jaenisch, R., and Brummelkamp, T.R. (2007). YAP1 increases organ size and expands undifferentiated progenitor cells. Curr. Biol. *17*, 2054–2060.

12. Bechmann, L.P., Hannivoort, R.A., Gerken, G., Hotamisligil, G.S., Trauner, M., and Canbay, A. (2012). The interaction of hepatic lipid and glucose metabolism in liver diseases. J. Hepatol. *56*, 952–964.

13. Rajeeve, V., Vendrell, I., Wilkes, E., Torbett, N., and Cutillas, P.R. (2014). Cross-species proteomics reveals specific modulation of signaling in cancer and stromal cells by phosphoinositide 3-kinase (PI3K) inhibitors. Mol. Cell. Proteomics *13*, 1457–1470.

14. Montoya, A., Beltran, L., Casado, P., Rodríguez-Prados, J.C., and Cutillas, P.R. (2011). Characterization of a TiO$_2$ enrichment method for label-free quantitative phosphoproteomics. Methods *54*, 370–378.

15. Cutillas, P.R., and Vanhaesebroeck, B. (2007). Quantitative profile of five murine core proteomes using label-free functional proteomics. Mol. Cell. Proteomics *6*, 1560–1573.